Rheology of Hydrate Forming Emulsions

Jorge Peixinho, Prasad U Karanjkar, Jae Ki Lee, Jeffrey F Morris

Rheology of Hydrate Forming Emulsions

Jorge Peixinho,[†,‡] Prasad U. Karanjkar,[†,‡] Jae W. Lee,[†] and Jeffrey F. Morris[*,†,‡]

Levich Institute and Chemical Engineering Department of City College of New York, New York, New York, 10031, USA

E-mail: morris@ccny.cuny.edu

May 20, 2010

Abstract

Results are reported on an experimental study of the rheology of hydrate forming water-in-oil emulsions. Density matched concentrated emulsions were quenched by reducing the temperature and an irreversible transition was observed where the viscosity increased dramatically. The hydrate forming emulsions have characteristic times for abrupt viscosity change dependent only on the temperature, reflecting the importance of the effect of sub-cooling. Mechanical transition of hydrate-free water-in-oil emulsions may require longer times, and depends on the shear rate, occurring more rapidly at higher rates but with significant scatter which is characterized through a probabilistic analysis. This rate dependence together with dependence on sub-cooling reflects the importance of hydrodynamic forces to bring drops or particles together.

Introduction

The formation of clathrate hydrates in water-in-oil (w/o) emulsions is a problem which may be encountered in subsea pipelines. Hydrates (gas hydrates or clathrate hydrates, among other terms ap-

[*]To whom correspondence should be addressed
[†]Chemical Engineering Department
[‡]Levich Institute

plied to these materials) are crystalline water-based solids physically resembling ice, but differing from ice in having small molecules trapped inside "cages" of hydrogen-bonded water molecules. Without the support of the trapped molecules, the lattice structure would collapse. Hydrates are thus compounds in which the host molecule is water and the guest molecule is a small molecule. The hydrate formation reaction leads to solidification of a fraction of the emulsion – with parts of the solid coming from both the aqueous and organic phases – and thus poses a problem because the change in properties of the flowing mixture may ultimately lead to flow stoppage or plugging.

The formation and decomposition mechanisms are still not well understood, but the thermodynamics for hydrate formation are well known.[1] Typically, hydrates are formed at temperatures below about 4°C in combination with elevated pressure in the range of 1-10 MPa. However, not all hydrate forming systems require elevated pressures and both cyclopentane (CP) and tetrahydrofuran (THF) form hydrates at atmospheric pressure at readily accessible temperatures. For example, the melting temperature of CP hydrate is approximately 7°C at atmospheric pressure.[2] This allows the study of hydrate formation processes without the added experimental difficulties of dealing with elevated pressure. Since THF is nearly fully miscible with water, the essential issue of mass transfer of the hydrate former (guest species) from the external organic phase to the water drops is not present in a THF-water system, whereas CP-water systems retain this feature seen in gas hydrate systems involving natural gas components, e.g. methane or propane. Note that when natural gas components are the guest molecules in a hydrate-forming emulsion, they are dissolved in the organic phase and undergo transport to the water drops.

Our study follows recent experimental studies which exploited the CP hydrate system[3–5] to develop understanding of hydrate formation processes without elevated pressure. Here we conduct cooling-controlled experiments, with the goal of revealing aspects of how the rheological properties of these mixtures change as the hydrate formation takes place. The background of this work thus involves both emulsion rheology as well as the thermodynamics and kinetics of the transformation to solid hydrate. Prior study of emulsions is extensive with some of the work reviewed by Mason.[6] Non-Newtonian rheology is expected because the deformable drop interactions depend

on the shear rate of the flow. Here, we focus on 40% concentrations of the internal phase as we seek to understand how aggregation may lead to bulk solidification of a hydrate-forming emulsion; similar behavior has been seen in our experiments at solid fractions as low as 20% water by volume.

Note that aggregation may be driven by inter-particle forces, settling, or by shearing flow. Guery et al.[7] investigated the shear activated aggregation of diluted double emulsion of water droplets dispersed in larger globules of crystallisable oil. Their double emulsion was prepared at 65°C and induction time for crystallization was observed to depend exponentially on the shear rate and the volume fraction. The dependence they observed was due to the hydrodynamic effects which control the particle aggregation. In another system, a suspension of polyvinyl chloride particles in plastisol (a resin) undergoing cooling and crystallization, Boudhani et al.[8] measured temperature dependence of the fluid and particle radii against time and concluded that these data could be the main inputs of a phenomenological model based on percolation laws. In the present investigation, temperature dependence of the fluid and time scales for the change in the physical properties of the materials are also measured for various temperature and flow conditions in order to extract further information about the irreversible transition.

At the drop scale, a puzzling question is: does the drop convert into ice or hydrates? The problem of converting a water drop into ice has been the subject of numerous works because of its implication in climatology. In an early series of experiments, Carte[9] found that individual droplets have freezing temperature depending on their size (diameter) and the cooling rate. In the case of water drops suspended within crude oil, Clausse et al.[10] also performed cooling experiments using differential scanning calorimetry (DSC) and proposed an empirical correlation between the size of droplets and their freezing temperature for a cooling rate of $1^{\circ}/\text{min}$. Both these studies found that the temperature required to convert an $O(1-10)$ μm diameter water drop into ice is in the range -30 to -40°C. Such surprisingly low temperatures are also found in nucleation experiments by Heneghan and Haymet[11] and Shaw et al.[12] whose findings also indicate that the time required to convert liquid water into ice increases with the cooling rate.

The observations noted above highlight issues of interest here, as we will consider cooling of emulsions containing water drops. Essential issues are whether the droplets convert into ice, hydrates, or a mixture of these, and how shear affects the conversion in CP-hydrate forming emulsions. This work will address these questions by investigating the rheology of water-in-oil emulsions with and without CP hydrate. The materials used in the study and the temperature dependence of their properties are presented in §2. In §3, rheological results over a wide range of shear and temperature conditions are given and compared for two systems before the conclusions in §4.

Experimental Section

Materials – The system studied here is a density-matched water-in-oil (w/o) emulsion. Matching of the oil and water phase densities at all temperatures studied is not possible in the experimental protocol followed, but by matching at room temperature very similar densities are maintained at all working temperatures to minimize segregation due to droplet sedimentation or rising.

The oil phase is a mixture of light mineral oil (from Fisher; density 850 $\mathrm{kg/m^3}$ at 25°C) and a polychlorotrifluoroethylene oil (Halocarbon 27; density 1,963 $\mathrm{kg/m^3}$ at 25°C). The temperature dependence of the viscosity of each liquid is given in Figure 1. The oil data were obtained from ramps of increasing and decreasing shear rate using a cone and plane or a Couette geometry; water viscosity results are from the International Organization for Standardization[13] and from the review by Debenedetti,[14] while the CP viscosity data are from Ma et al.[15] The viscosity for each material can be fitted by an Arrhenius form: $\mu(T) = A\exp(E/RT)$ where the temperature is in Kelvin, and $R = 8.314\ \mathrm{J.K^{-1}.mol^{-1}}$ is the gas constant. The values of the coefficients A and E for the different materials are given in Table 1. Large values of E indicate the oil viscosities are more sensitive to temperature than water or CP. In the case of the light mineral oil at $T < -15$°C, it is observed that the scatter of viscosity increases associated with the formation of wax crystals. Note that that all the experiments analyzed in this study are in the range -10 to 25°C, hence well above -15°C. So the oils will remain liquid although very viscous as quantified in Figure 1. For the Halocarbon oil, the pour point is -40°C.

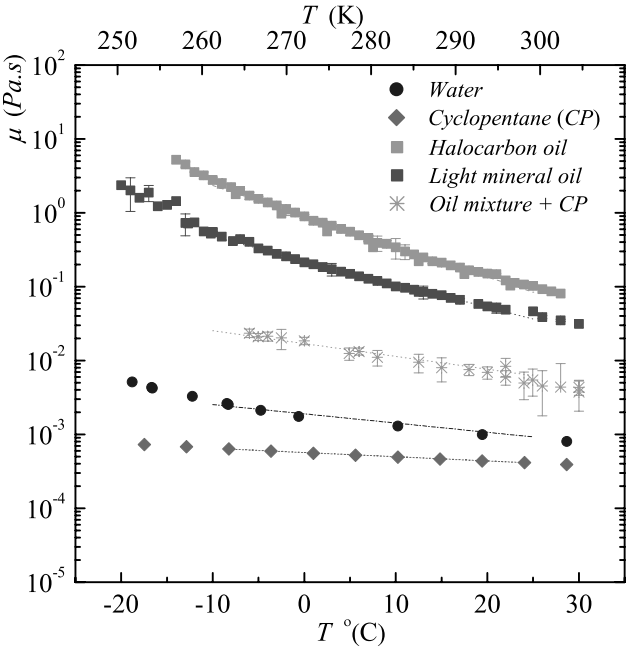

Figure 1: Shear viscosity versus temperature for the Halocarbon oil, the light mineral oil, the density matched CP-oil mixture, the standard and sub-cooled water, and the CP. Water data from [13] and Debenedetti; [14] CP data from Ma et al. [15] The lines represent fits in the working range, i.e. -10 to 25°C (263.15 to 298.15 K), and the coefficients are given in Table 1.

A non-ionic surfactant, sorbitan monooleate, commercially known as Span 80 (Fluka), is used. Its chemical formula is $C_{12}H_{44}O_6$, with molar mass of 428.62 g/mol and density is 986 kg/m^3. The hydrophilic-lipophilic balance [16] is 4.3$\pm$1.0 at 25°C (according to the distributor).

Cyclopentane, C_5H_{10}, (Acros Organics) is used as a hydrate former. Its density is 751 kg/m^3. All the materials in this study are used as received without further purification. De-ionized water is used as the internal phase and it is obtained from a Millipore QTM water purification system. The viscosity ratio between the oil phase and the water ranges between 50 to 3,000 in this work, depending on temperature and the system studied.

Table 1: A and E values from the viscosity fits $\mu(T) = A\exp(E/RT)$ in Figure 1 for the Halocarbon oil, light mineral oil, water and CP in the working range -10 to 25°C (263.15 to 298.15 K).

	A (Pa.s)	E (J.mol^{-1})
Halocarbon Oil	1.67×10^{11}	11.4
Light Mineral Oil	1.12×10^{8}	8.81
Water	4.64	3.46
CP	0.015	1.46

Preparation – The oil mixture is prepared first. Then Span 80 surfactant is added at a concentration of 0.05% in volume. Our pendant water drop tests in light mineral oil indicate the critical micelle concentration is around 0.01%, which agrees satisfactorily with data from previous experiments by Opawale and Burgess.[17] The surface tension at this condition is slightly below 5 mN/m. The two phases are mixed and mechanically stirred in a 45 mm diameter beaker with a three blade agitator at 500 rotations per minute for 5 minutes. The emulsions are stable against coalescence under quiescent conditions for several hours. However, at small shear rates, i.e. $O(0.1)$ s^{-1}, and long times (few hours), some shear induced flocculation is observed.

Two systems, both with 40% water volume fraction, are studied. The first system is a "simple" w/o emulsion which is only the mixture of oils, the Span 80 surfactant and the deionized water. The second one is a CP emulsion in which the oil phase contains 50% by volume of CP. Both the systems have a fixed fraction of surfactant, 0.05% by volume of the oil phase. The stoichiometric CP to water molar ratio for complete conversion to hydrate is about 1:17 according to Zhang et al.,[5] so CP is in excess for the hydrate formation reaction.

Protocol – A rapid temperature quench is performed. The emulsion is prepared at room temperature and gently transferred to the rheometer where the temperature was previously set to the low working temperature. The stainless steel outer walls of the Couette cup are in contact with the cooling re-circulating fluid. During the runs, the rheometer tool is covered and is within an insulating foam enclosure in order to minimize heat transfer from the surroundings. Owing to the laminar Couette flow, the temperature distribution in the flow is determined primarily by thermal diffusion. The diffusion time for transfer across the rheometer gap of 2 mm (see below for the full geometry) is estimated to be approximately 20 s; for longer time the temperature is expected to be equilibrated within the Couette gap.

Drop size distribution – The drop size distribution is obtained by optical microscopy. A fresh sample of an emulsion was transferred into a rectangular glass tube (0.1×1 mm). In the case of CP emulsion, the transfer induced drop-drop coalescence. An alternative approach[18] to this problem,

presumably due to the nature of the microscope glass slides, consists in transferring the prepared emulsion in a 0.1% Span 80 solution, without additional stirring to avoid drop size change. The sample of the stabilized emulsion was used for the analysis.

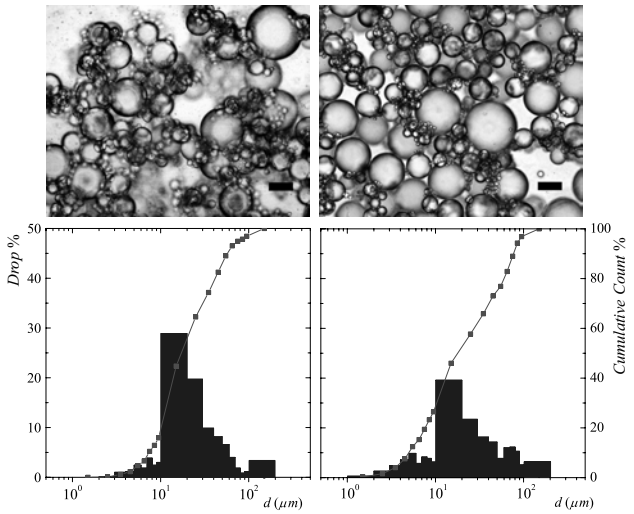

Figure 2: Photomicrograph and histograms of the drop diameter. The bars on the photomicrographs represent 100 micrometers. Left: simple w/o; right: CP w/o.

Photomicrographs and drop size distribution histograms are presented in Figure 2. For each system, 700 drops are analyzed. For the simple system, the average drop size is 34.5 μm and the standard deviation is 30.3 μm. For the system containing CP, the average drop size is 30.5 μm and the standard deviation is 25.3 μm.

Rheology – The rheological data were obtained using an ARES controlled strain rheometer equipped with a Couette geometry having cup diameter of 34 mm, cylinder diameter of 32 mm, and cylinder length of 33.5 mm. The temperature is set using a cooling bath and monitored with a thermocouple placed at the bottom of the cup. Note that tests are conducted with approximately 15 milliliter samples. Additional tests were conducted using a vane geometry consisting of 6 blades corresponding to an inner diameter of 18 mm. When using the vane, the sample volume is about 40 ml.

Shear viscosity – Figure 3 presents the shear viscosity of the emulsions for different temperatures. As expected from the results of Figure 1, the viscosity increases with a lowering of the temperature. Each shear ramp curve is the result of an average of 2-4 ramps and the error bars represent the scatter of the results. For the CP emulsion, the errors bars are very large. The viscosity measured seems to be very sensitive to initial conditions of the experiments. The simple emulsion is more viscous than the CP emulsion reflecting the effect of the lower viscosity of the oil phase. The emulsions exhibit a shear thinning behavior, with viscosity of form $\eta \sim \dot{\gamma}^{n-1}$, where the shear thinning index is $n = 0.9$ for the simple w/o system, and $n = 0.7$ for the CP emulsion.

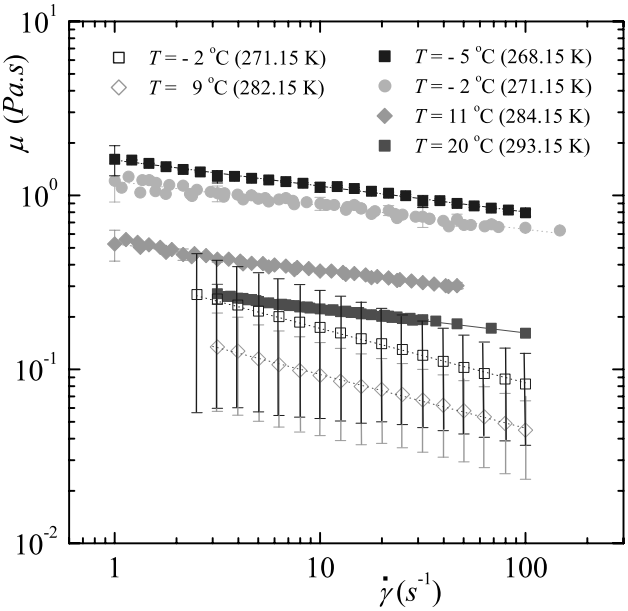

Figure 3: Viscosity versus shear rate of the w/o emulsion at different temperature. Filled symbols are for simple w/o emulsions and open symbols are for the CP emulsions.

Results and Discussion

The results are mainly presented as functions of time. In a first part, the statistics of the time-varying material property changes for the simple emulsion at different temperatures and shear rates are described and analyzed. In a second part, the results for the CP emulsion are presented and analyzed. In a third part, linear visco-elastic results are presented, which confirm the shear experiments. Finally, features of the final material and tests conducted using a vane geometry are

discussed.

Simple w/o emulsions

Critical time – The emulsion is prepared at room temperature, inserted in the Couette device at working temperature and set into motion. The viscosity first increases slightly due to temperature effects, then stays constant until a critical time t_c, whereupon it rapidly increases typically by almost a factor 10. This dramatic measured viscosity change is qualitatively reproducible, but not at the same t_c value. However, for a set of ten runs, we obtained the range of critical times. When inspecting the results at different shear rates and different temperatures, available in the supplementary information, the dramatic increase is again about one order of magnitude in viscosity over a large range of shear rates and temperatures.

It is not possible to account for the change in viscosity due only to a change from liquid to solid of the dispersed phase. Such a change for moderate internal phase fractions results in an $O(1)$ change in viscosity, and we observe an increase by about one order of magnitude. While the expressions do not apply to the 40% emulsions studied here, the point can be appreciated by comparing the dilute system expression for a suspension, Einstein expression $\mu_e = \hat{\mu}\,(1+2.5\phi)$ for rigid spheres to the expression by Taylor[19] for the emulsion, $\mu_e = \hat{\mu}\left(1+\phi\frac{5\lambda+2}{2\lambda+2}\right)$ which gives the effective viscosity of a dilute emulsion with large interfacial tension such that the droplets remain nearly spherical. Here, ϕ is the internal phase volume fraction and $\lambda = \mu'/\hat{\mu}$, where μ' and $\hat{\mu}$ are the viscosities of the droplets and the matrix respectively. When the internal phase is of very low viscosity as in our work, the viscosity increment is a factor of 2.5ϕ for the suspension as opposed to ϕ for the emulsion. Clearly, the transition from emulsion of spheres to a suspension of rigid spheres cannot explain the large increase observed. Some other physical phenomenon is responsible of the dramatic increase.

Experimental data at three different temperatures and three different shear rates have been performed so the cumulative critical time probability $P(t_c)$ can be measured. A value of $P = 0$ means that the large viscosity increase did not occur in any cases at this time, and $P = 1$ means

the irreversible transformation occurred in all cases by this time. A figure of $P(t_c)$ is shown in the supplementary information. Another measure which can be extracted from the probability is the time required for half the experiments to exhibit the abrupt viscosity increase, $t_{1/2}$. Hence $t_{1/2}$ is presented as a function of the shear rate for different temperature in Figure 4(a). The error bar indicates the scatter. It is observed that for high shear rate, the critical time is short and tends to be independent of temperature. There is a rapid decrease of the critical time when the shear rate increases from $\dot{\gamma} = 1$ to 100 s^{-1}. For small shear rate, the error bars are very large; it is possible that wall slip occurs and is responsible for the scatter in the measurements.

At high shear rate, the drop capillary number, Ca, i.e. the ratio between the capillary forces and the viscosity forces, can be estimated to be at most $Ca = \mu\dot{\gamma}d/\sigma = O(10^{-1})$, whereas for low shear rate $Ca = O(10^{-3})$. In this range of Ca, there are studies[20–23] on collision of pairs of drops, which indicate flow-induced drop deformations and coalescence. Specifically, Baldessari and Leal[22] indicate that the non-dimensional drainage time scales roughly as $Ca^{3/2}$ and this exponent varies slightly with λ. Moreover, the surfactant molecules at the interface inhibit coalescence in the sense that the time required for film drainage up to rupture is increased. This drainage time could be related to the transition time to the dramatic transition t_c. In Figure 4(b), the non-dimensional time $t_c\dot{\gamma}$ is represented as a function of Ca and the lines are power law fit with exponent of 0.4 to 0.7. The discrepancy between the observed exponent (0.4 to 0.7) and the exponent found in coalescence of drop in theoretical and numerical studies[20–23] suggests that drainage and coalescence are not the primary mechanism here to explain the formation of the ice slurry.

Moreover, sampling and low temperature microscopy of the ice slurry shown in the inset of Figure 4(b) indicate that the transition is associated with the existence of clusters of ramified particles. The clusters are very reminiscent of those observed in previous studies on aggregation phenomena in similar w/o emulsions[24] and their size is of $O(100)$ μm, whereas the drop are initially around 30 μm. Hence the temperature decrease leads to aggregation. However, the formation of a solid material apparently plays a role as well.

The product following the transition is an ice slurry material. When the temperature is raised

above 0°C, the ice slurry melts into a destabilized emulsion with a few very large water drops.

CP w/o emulsions

Now we consider the results for the emulsion in which the oil phase contains CP. There are several evidences of hydrate growth. The most clear signature of hydrate formation is that the solidified rigid material did not melt at a temperature of 0° C but at a higher temperature between 4 and 5°C in agreement with our and other micro-DSC studies of the hydrate equilibrium temperature in this system.[2,4,5]

Critical time – Again quench experiments of sheared emulsions show a large viscosity increase. Results for three sub-cooling temperature and four shear rates are available in the supplementary information. In all the CP emulsion runs, the transition manifests by a systematic increase of the viscosity by several orders of magnitude. This suggests that the interactions within the material are much stronger than in the simple emulsion case. It is interesting to notice the large scatter is observed at the beginning of the test, possibly due to slip at the wall, heat transfer effects, or sensitivity to the initial conditions. Also, the large scatter observed at the final state seems to be associated with slip and therefore the actual value of the viscosity is probably not meaningful, except to indicate the material has become dramatically more efficient in stress transmission.

Figure 5 presents $P(t_c)$ at several shear rates for the CP-hydrate forming emulsion. Again, there is a definite range of times which can be extracted from these probability measurements. The location for the large viscosity increase is controlled by the temperature, i.e. the level of sub-cooling relative to the equilibrium temperature for the CP hydrate.

As expected, the half-life critical time, $t_{1/2}$ increases with the temperature. The figure is available in the supplementary information. More importantly, there seems to be no dependence on the shear rate: unlike the simple ice-forming emulsion, the shear rate has little effect on t_c in the hydrate-forming emulsion for the range of parameters studied. Here the Ca is in the range $O\left(10^{-6} - 10^{-2}\right)$ because of the lower viscosity of the matrix. The critical times are of a smaller

magnitude than in the case of the first system and also the error bars on the critical times are smaller. This better reproducibility is due to the large subcooling experienced by the CP hydrate emulsion.

Linear visco-elasticity

The previous results on the critical time from shear viscosity of the CP emulsions seem to indicate that shear has no effect on the rapid transformation of these hydrate-forming emulsion properties. In order to confirm that the critical time is independent of shear rate, linear visco-elastic measurements are performed. These tests applied a very small strain $\gamma = 0.05\%$ at a constant frequency of 1 Hz and observed the mechanical response as a function of time. Figure 6(a) represents the dynamic elastic modulus, G', as a function of time for different temperature steps. As expected, the CP w/o emulsion experiences the dramatic change in the material properties at time of about 600 seconds for a the temperature of $-8.6°$C, whereas a simple w/o requires typically over 10^4 seconds (or 3 hours) before the material transition is observed. A comparison between the simple emulsion and the CP emulsion is available in the supplementary information. Then at $t = 1500$ s, the temperature is raised to a constant value $T = 1°$C, where ice melts. This temperature is maintained for 30 minutes, so that all the ice is expected to melt but hydrate can grow. Initially, G' increases and then stays constant during the 1°C plateau indicating that the sample is rigid and can only be an hydrate block within the geometry gap. From $t = 4100$ s, T increases to 20°C. Hydrate dissociation is observed at a temperature of 5°C in agreement with literature values.[2,4,5] Prior to the dissociation, a reproducible G' increase is observed. After the dissociation, G' has small values corresponding to a destabilized emulsion.

Additional linear visco-elastic measurements were conducted using a vane geometry (described earlier). When using the vane, the sample volume is almost tripled to about 40 ml. However, no significant change in the critical time was observed. Figure 6(b) is a photograph after the transition at the end of a typical test. It shows a rigid hydrate block. Whereas the simple emulsion undergoing similar temperature evolution forms a non-Newtonian ice slurry.[25,26]

Conclusions

Temperature quench experiments on the rheometric Couette flow of emulsions have been carried out. A simple 40% internal phase density-matched w/o emulsion was designed and used together with a w/o emulsion containing CP, an atmospheric pressure hydrate former, at the same internal phase fraction. The main conclusion of our measurements is related to the effect of critical time on the dramatic shear viscosity and visco-elasticity increase occurring during this dynamic phase change. The CP loaded w/o emulsion is more sensitive to the sub-cooling temperature than to the shear rate. The onset of a mechanical transition in a hydrate-free water-in-oil emulsions may take longer times, and depends on the shear rate as well as sub-cooling. We conclude that a flow process, involving hydrodynamic forces driving the drops together as well as aggregation, are at play in the transition for this system.

For the simple w/o emulsion, our results indicate the ice is absent prior to the sudden change in the material properties. There is evidence indicating an aggregation process leading to the dramatic material properties change. The emulsions containing CP hydrates in the oil phase have an abrupt viscosity change dependent on the temperature only reflecting the importance of the chemical kinetics and the degree of subcooling of the hydrates.

Acknowledgements. The authors acknowledge support from Chevron and discussions with the Chevron Flow Assurance Core Team.

Supporting Information Available: Additional figures. This material is available free of charge via the Internet at http://pubs.acs.org

References

(1) Sloan, E. D. *Clathrate hydrates of natural gases*; CRC Press, Taylor and Francis Group, 1980.

(2) Zhang, J. S.; Lee, J. W. *J. Chem. Eng. Data* **2009**, *54*, 659-661.

(3) Lo, C.; Zhang, J. S.: Somasundaran, P; Lu, S.; Couzis, A.; Lee, J. W. *Langmuir* **2008**, *24*, 12723-12726.

(4) Nakajima, M.; Ohmura, R.; Mori, Y. H. *Ind. Eng. Chem. Res.*, **2008**, *47*, 8933-8939.

(5) Zhang, Y.; Debenedetti, P. G.; Prud'homme, R. K.; Pethica, B. A. *J. Phys. Chem. B* **2004**, *108*, 16717-16722.

(6) Mason, T. G. *Curr. Opin. Colloid Interface Sci.* **1999**, *4*, 231-238.

(7) Guery, J; Bertrand, E.; Rouzeau, C.; Levitz, P.; Weitz, D. A.; Bibette, J. *Phys. Rev. Lett.* **2006**, *96*, 198301.

(8) Boudhani, H.; Fulchiron, R.; Cassagnan, P. *Rheol. Acta* **2009**, *48*, 135-149.

(9) Carte, A. E. *Proc. Phys. Soc. Lond. B* **1956** *69*, 1028-1037.

(10) Clausse, D.; Gomez, F.; Dalmazzone, C.; Noik, C. *J. Colloid Interface Sci.* **2005**, *287*, 694-703.

(11) Heneghan, A. F.; Haymet, A. D. J. *J. Chem. Phys.* **2002**, *117*, 5319-5327.

(12) Shaw, R. A.; Durant, A. J.; Mi, Y *J. Phys. Chem. B* **2005**, *109*, 9865-9868.

(13) International Organization for Standardization, *Viscosity of water* Technical Report 3666; 1999.

(14) Debenedetti, P. G. *J. Phys.: Condens. Matter* **2003**, *15*, R1669-R1726.

(15) Ma, R.-F; Duan, Y.-Y.; Han, L.-Z.; Liu, N.-X. *J. Chem. Eng. Data* **2003** *48*, 1418-1421.

(16) de Gennes, P. G.; Brochard-Wyard, F.; Quere, D. *Capillary and wetting phenomena: drops, bubbles, pearls, waves*; Spinger, 2004.

(17) Opawale, F. O.; Burgess, D. J. *J. Colloidal Interface Sci.* **1998** *197*, 142-150.

(18) Tcholakova, S.; Denkov, N. D.; Danner, T. *Langmuir* **2004** *20*, 7444-7458.

(19) Taylor, G. I. *Proc. Roy. Soc. Lond. A* **1932**, *138*, 41-48.

(20) Loewenberg, M.; Hinch, E. J. *J. Fluid Mech.* **1997** *338*, 299-315.

(21) Leal, L. G. *Phys. Fluids* **2004** *16*, 1833-1851.

(22) Baldessari, F.; Leal, L. G. *Phys. Fluids* **2006** *18*, 013602.

(23) Dai, F.; Leal, L. G. *Phys. Fluids* **2008** *20*, 040802.

(24) Leal-Calderon, F.; Gerhardi, B.; Espert, A.; Brossard, F.; Alard, V.; Tranchant, J. F.; Stora, T.; Bibette. J.; *Langmuir* **1996**, *12* 872-874.

(25) Ayel, V.; Lottin, O.; Peerhossaini, H. *Int. J. Refrigeration* **2003** *26*, 95-107.

(26) Stokes, J. R.; Telford, J. H.; Williamson, A.-M. *J. Rheol.* **2005** *49*, 139-148.

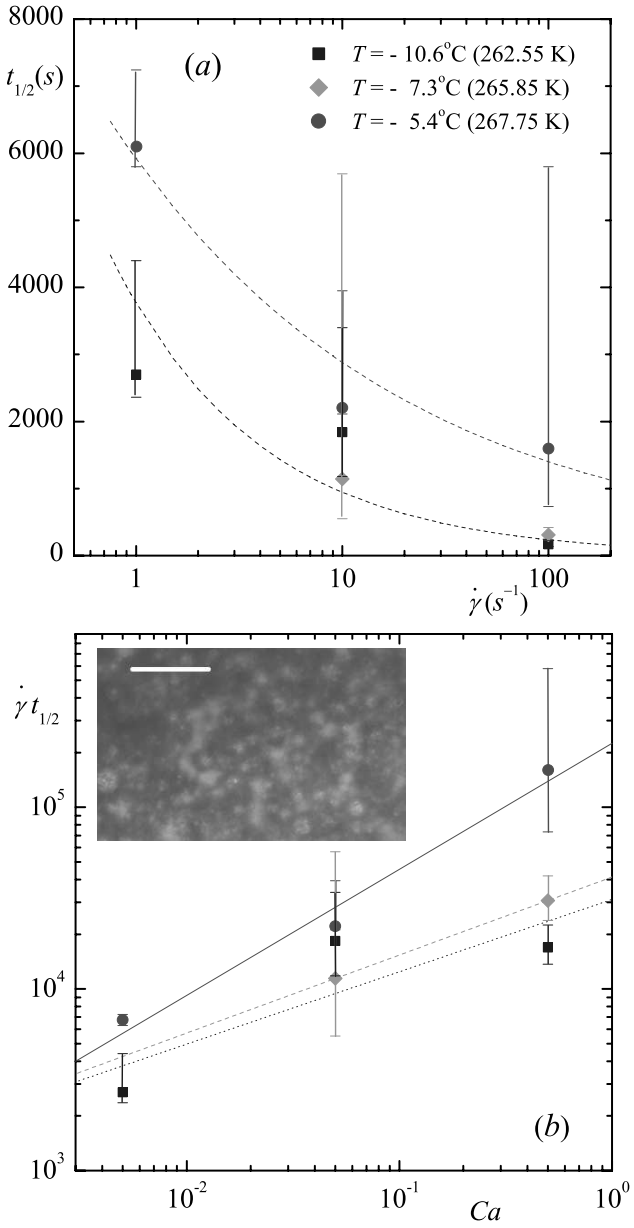

Figure 4: (*a*) Time for the most probable t_c or $t_{1/2}$ for the simple emulsion as a function of shear rate, $\dot{\gamma}$, and for several T. (*b*) Non-dimensional time, $\dot{\gamma}t_{1/2}$, versus Ca. The lines represent power law fit described in the text. The inset in (*b*) is a photomicrograph of the ice slurry aggregates observed under low temperature microscope. The scale bar represents 0.5 mm.

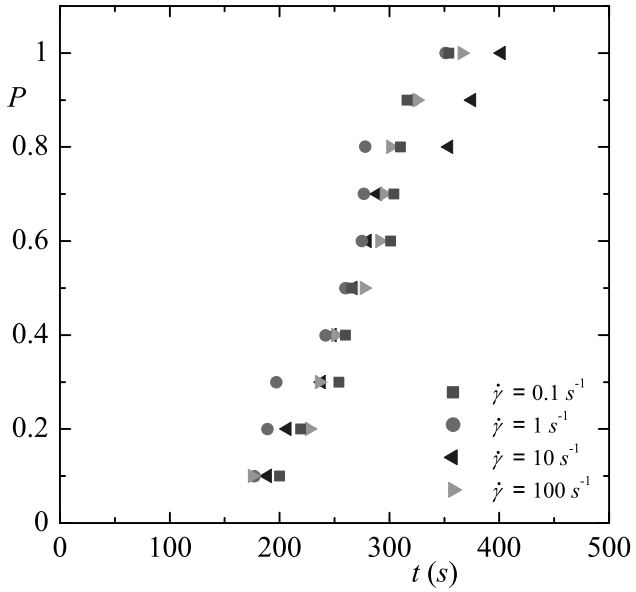

Figure 5: Critical time probability for the CP emulsion as a function of time for $T = -6.3 \pm 0.5$°C (266.85 K) and for 4 different shear rate values $\dot{\gamma} = 0.1,\ 1,\ 10$ and 100 s^{-1}.

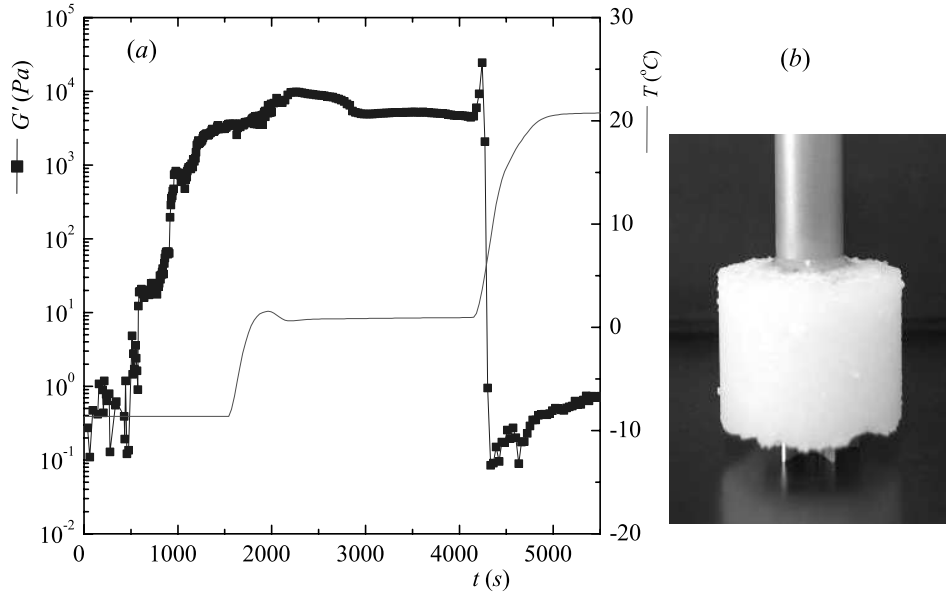

Figure 6: (*a*) G' versus time for a CP emulsion undergoing the quench and temperature steps at 1°C and 20°C in the Couette geometry. (*b*) Hydrate block or end product from a thermal quench to -10°C (263.15 K) for the CP hydrate-forming emulsion in the vane geometry. The outside diameter is 34 mm.

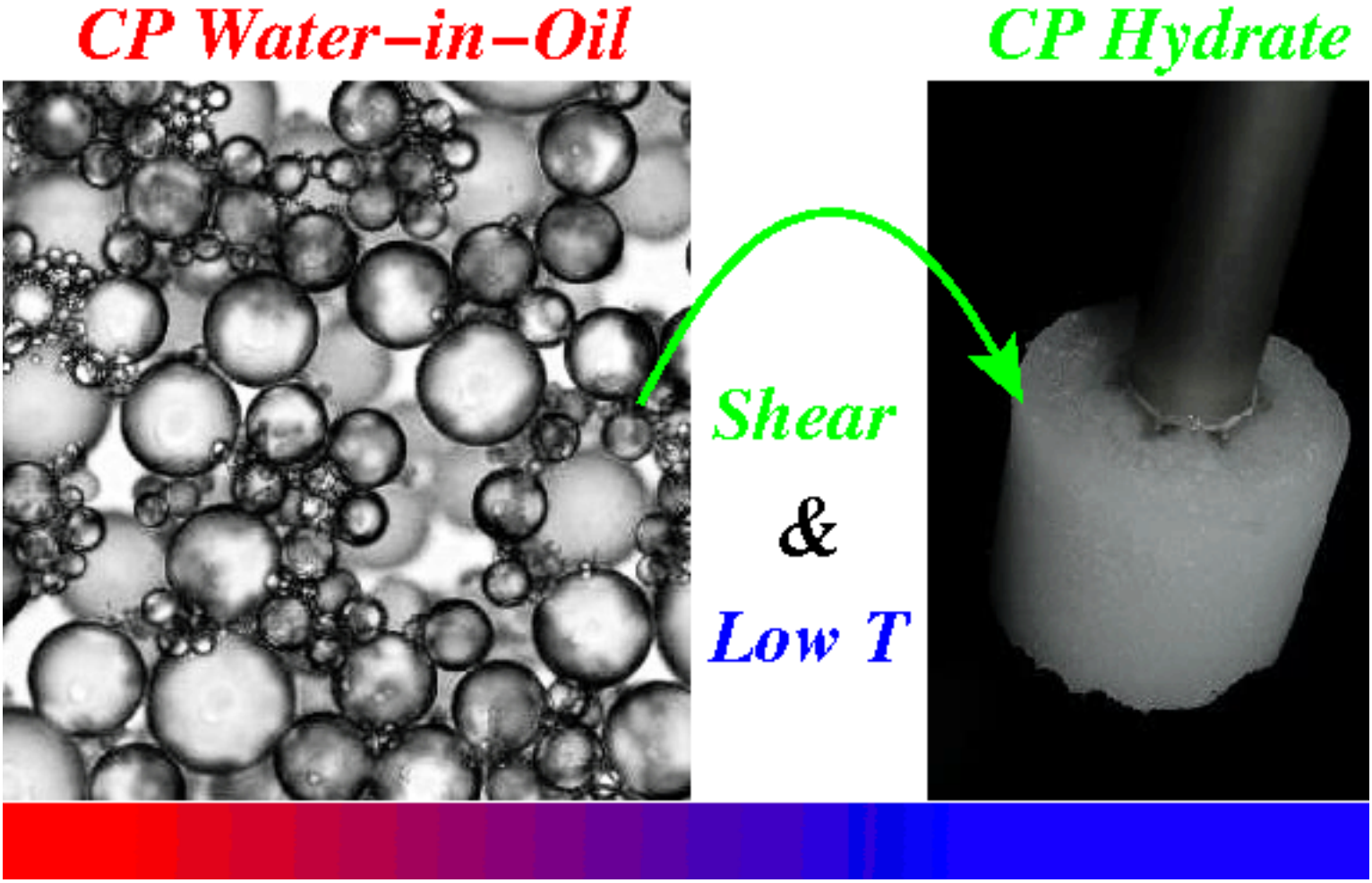
CP Water–in–Oil
CP Hydrate
Shear
&
Low T

Supporting Information

Rheology of Hydrate Forming Emulsions

Jorge Peixinho,[†, ‡] Prasad U. Karanjkar,[†, ‡] Jae W. Lee,[†], and Jeffrey F. Morris[*, †, ‡]

[†] Levich Institute, City College of New York, New York, New York, 10031, USA
[‡] Chemical Engineering Department, City College of New York, New York, New York, 10031, USA
[*] E-Mail: morris@ccny.cuny.edu

The figures S1 to S6 below show the evolution of the mixture rheology in a Couette geometry with a narrow gap for a non-hydrate forming water-in-oil emulsion (termed a simple w/o emulsion) as well as a CP-hydrate forming w/o emulsion, as described in the manuscript.
These are shown for different temperatures, all below the ice melting or hydrate dissociation equilibrium temperature, and different shear rates. The different curves for each condition simply represent the variability of the process, as each mixture is prepared by the same protocol, as described in the manuscript.

The figure S7 shows $P(t_c)$ for the simple emulsion at a working temperature T = -10.6^{o}C. Each curve represents the results of 10 runs at the stated shear rate. For high shear rate, i.e. 100 s^{-1}, the conversion of the emulsion into ice slurry occurs faster; t_c is typically less than 300 seconds. Then, decreasing the shear induces an increase of t_c.

The figure S8 shows the evolution of $t_{1/2}$ of the CP emulsion as a function of shear rate and the temperature.

The figure S9 is linear visco-elasticity measurements for both the simple emulsion and the CP emulsion. It confirms the CP-hydrate forming emulsion is sensitive to sub-cooling temperature only, whereas the simple emulsion requires much longer times for transition.

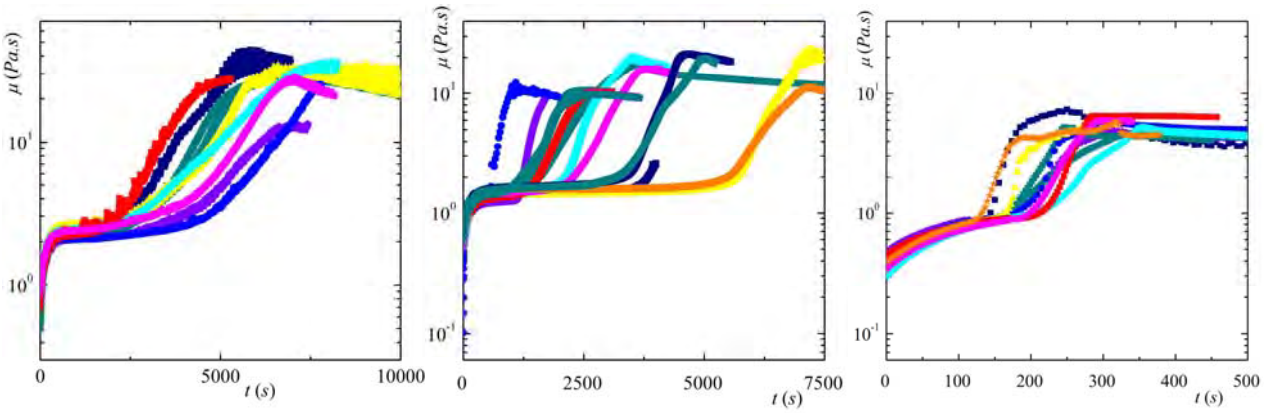

Figure S1: T = -10.6±0.6°C. μ versus time of the simple emulsion for shear rates of 1, 10 and 100 s^{-1}.

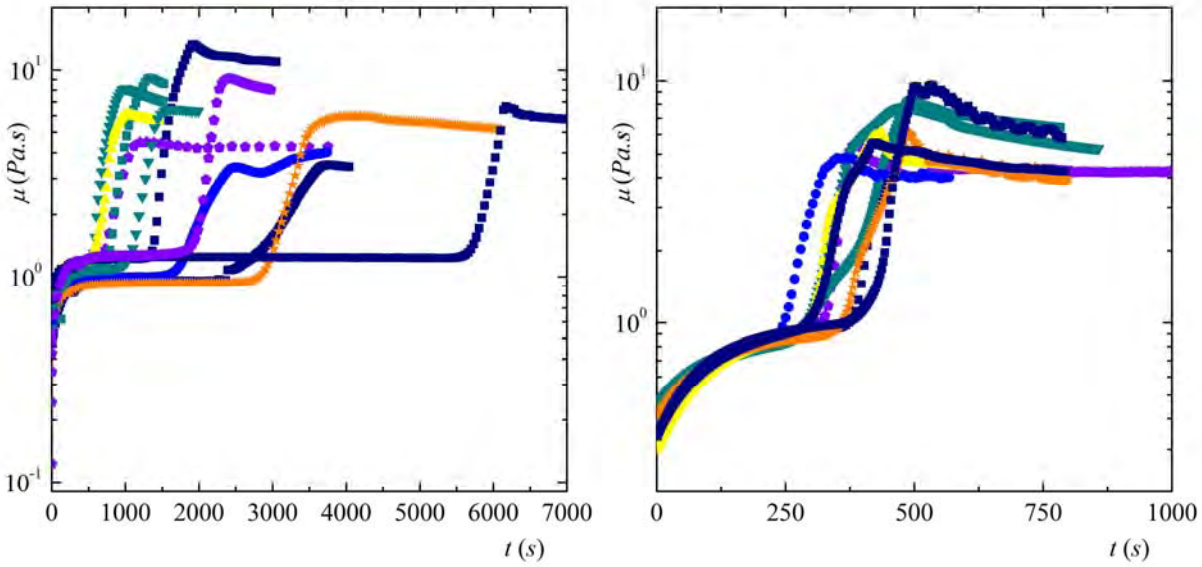

Figure S2: T = -7.3±0.6°C. μ versus time of the simple emulsion for shear rates 10 and 100 s^{-1}.

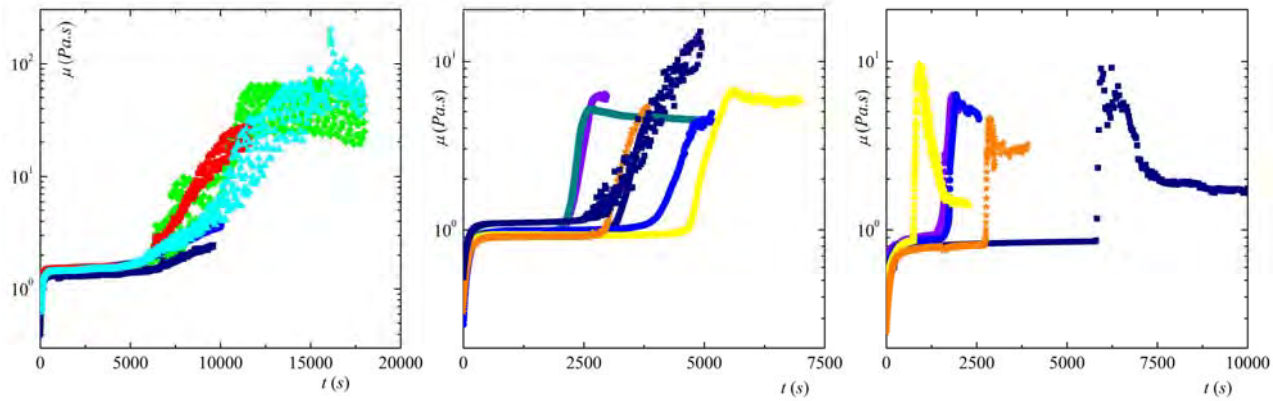

Figure S3: T = -5.4±0.6°C. μ versus time of the simple emulsion for shear rates 1, 10 and 100 s^{-1}.

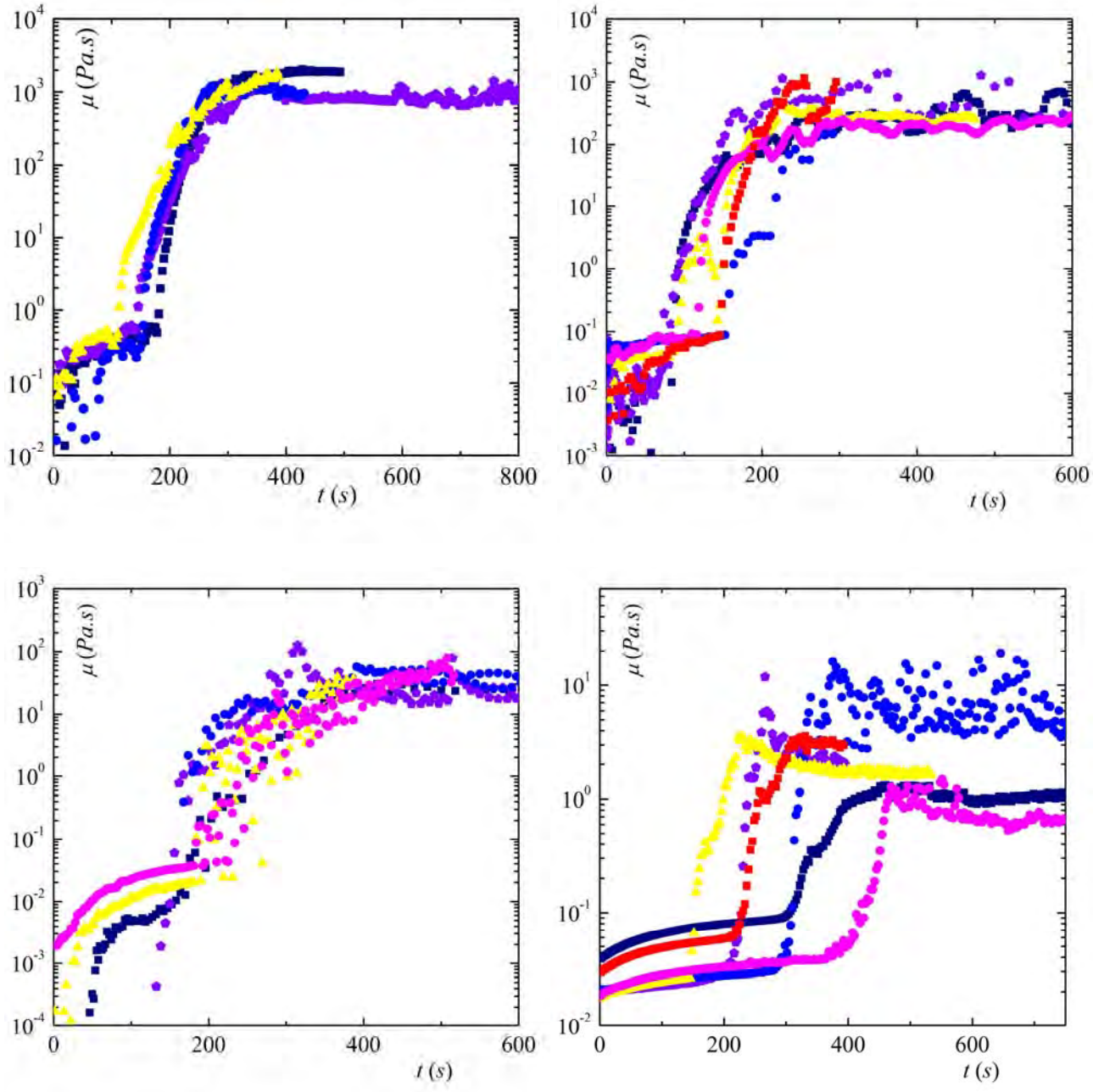

Figure S4: T = -9.8±0.6°C. μ versus time of the CP emulsion for shear rates 0.1, 1, 10 and 100 s^{-1}.

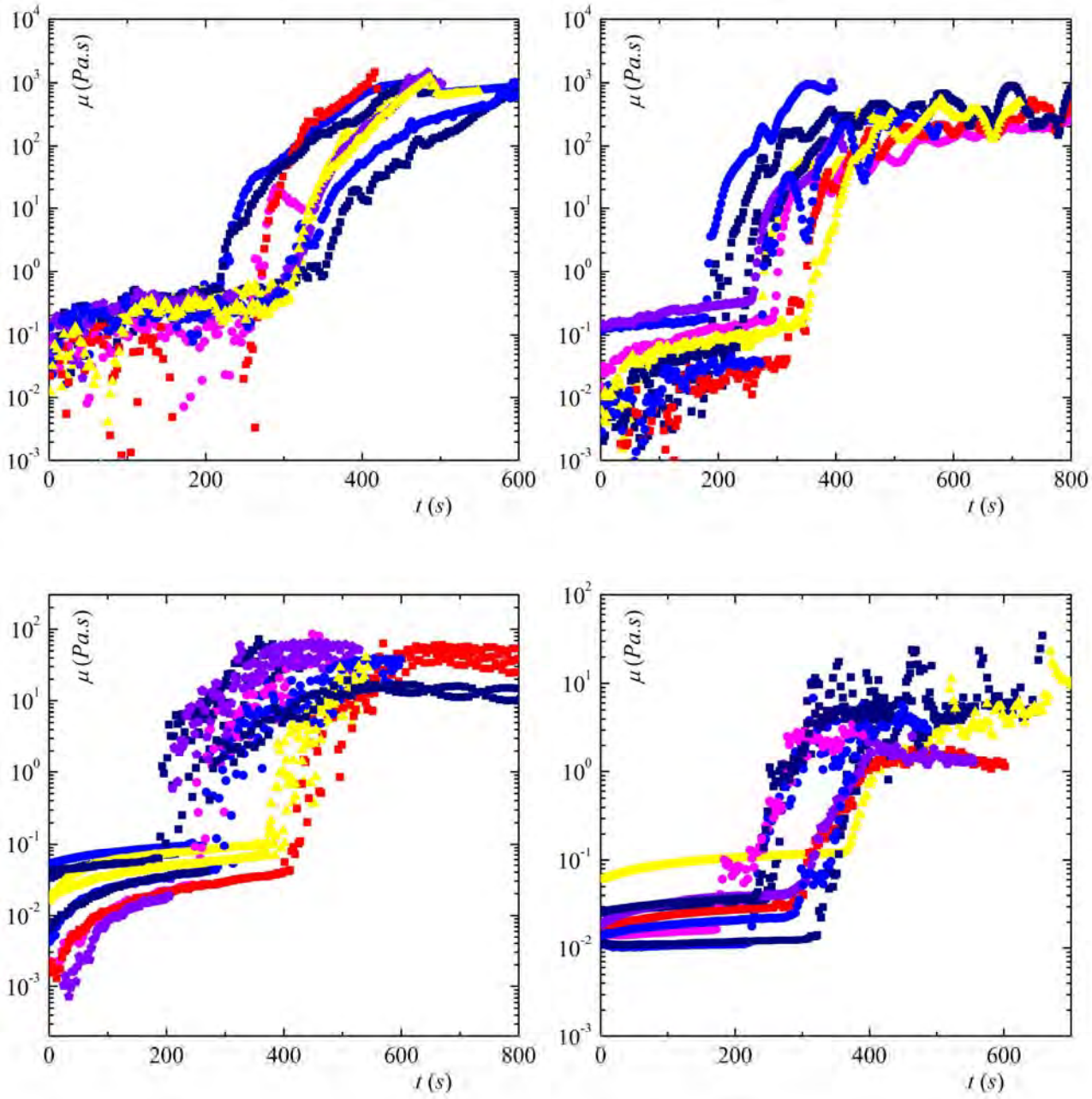

Figure S5: T = -6.3±0.6°C. μ versus time of the CP emulsion for shear rates 0.1, 1, 10 and 100 s^{-1}.

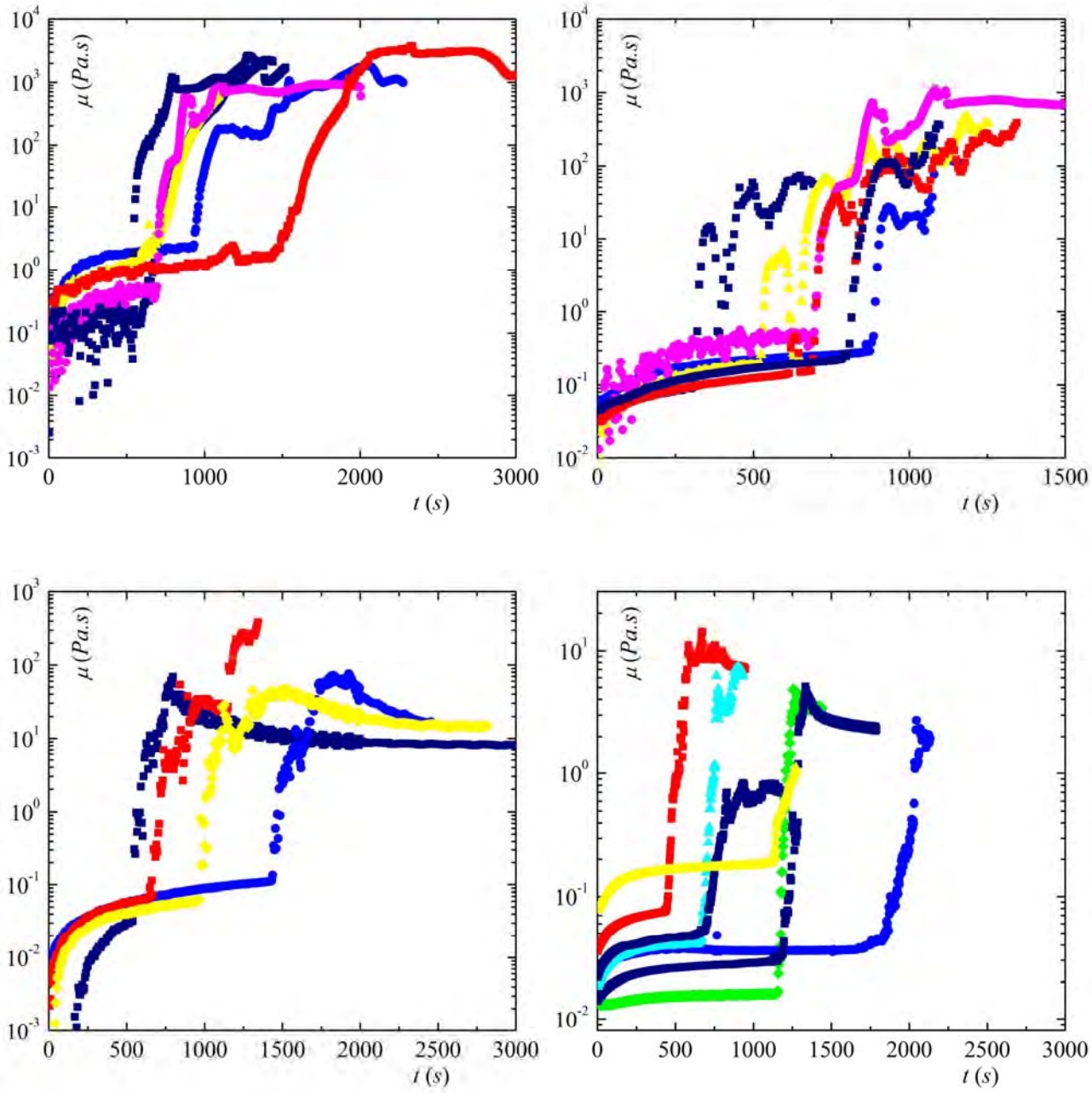

Figure S6: T = -5.3±0.6°C. μ versus time of the CP emulsion for shear rates 0.1, 1, 10 and 100 s^{-1}.

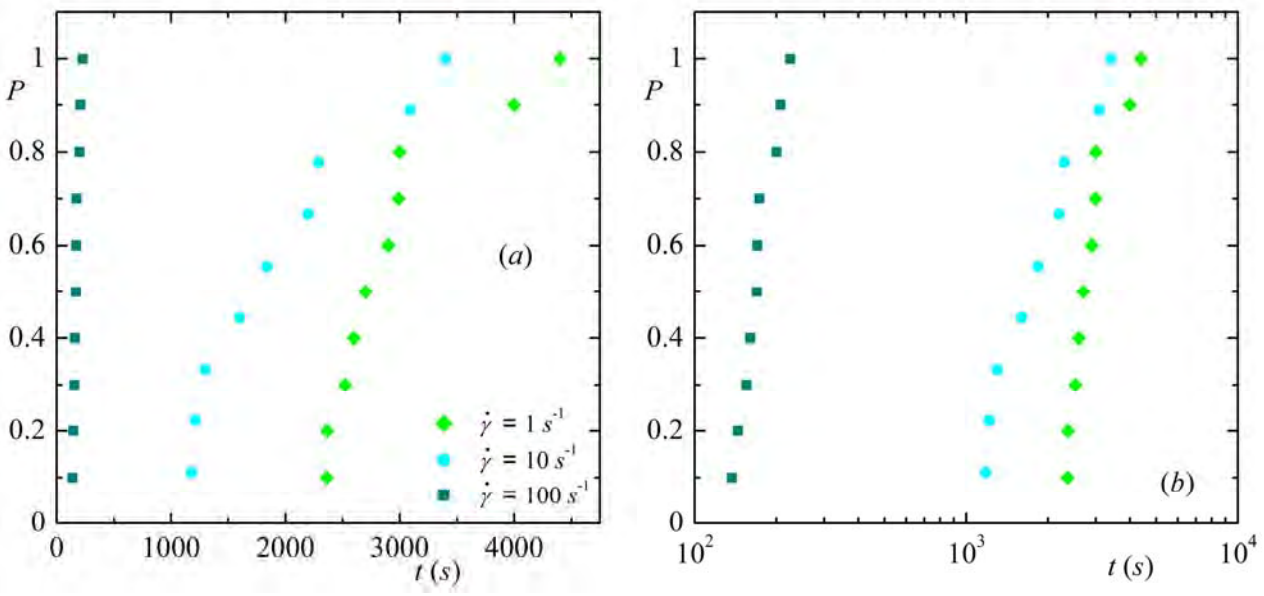

Figure S7: Critical time probability for the simple emulsion as a function of time for T = -10.6±0.6°C (262.55 K). (*a*) $P(t)$ with time on a linear scale and (*b*) $P(t)$ with time on a log scale.

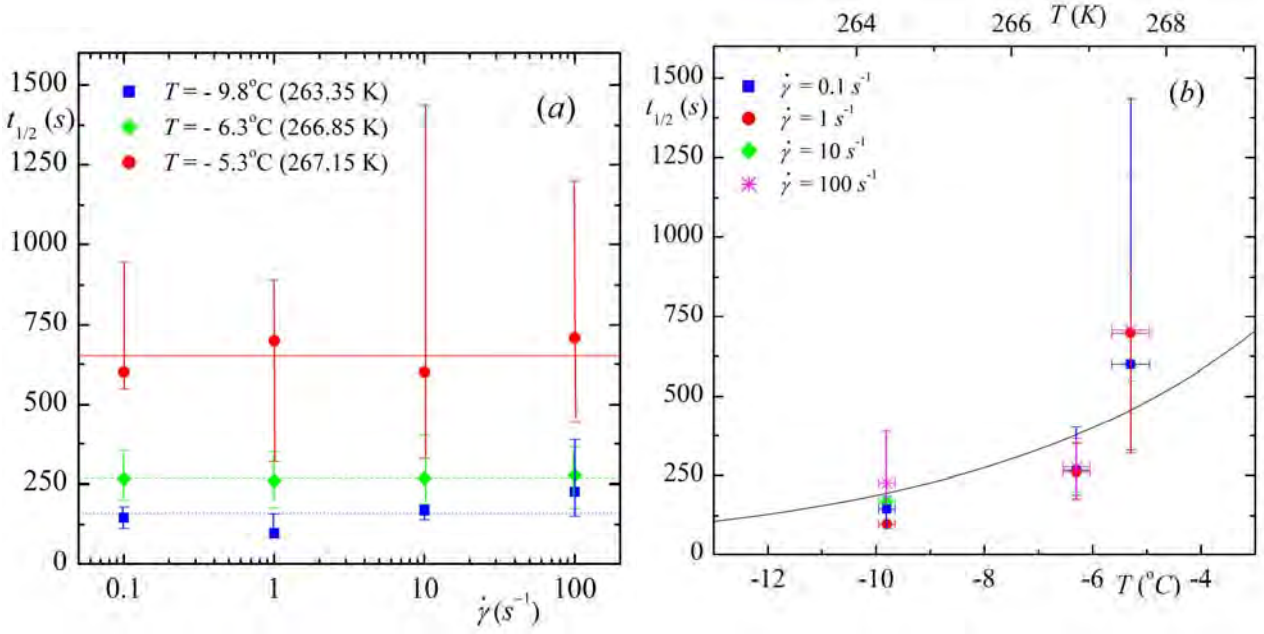

Figure S8: (*a*) $t_{1/2}$ for the CP emulsion versus shear rate. (*b*) $t_{1/2}$ versus T and the line represent a fit with indicates a rapid increase of the critical time with increasing working temperature, suggesting the expected divergence as the equilibrium temperature is approached. The line is a fit of the form $t_{1/2} \propto (T^* - T)^{\alpha}$, where T^* is the CP melting temperature and α is the exponent.

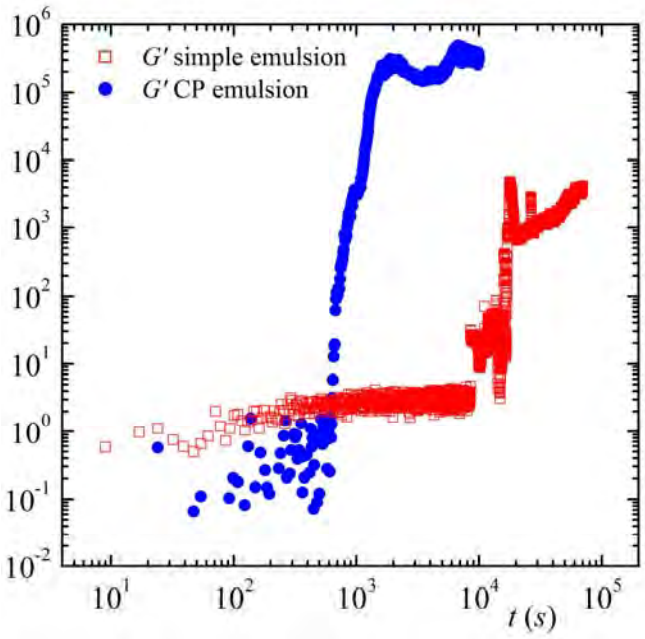

Figure S9: Linear visco-elastic measurements at a strain of 0.05% and frequency 1 Hz in the Couette geometry: *G'* versus time for both the 40% simple emulsion and the CP emulsion at T = - 6.3^{o}C.